Performance Assessment of Newly Designed Solar Water Treatment System

Mukesh Kumar Gupta * ⓘD , Krishna Kumar Sinha**‡ ⓘD , Rahul Kumar ***‡ ⓘD , M. K. Banerjee**** ⓘD

* Department of Energy and Electrical Engineering, Suresh Gyan Vihar University, Jaipur-302017 India

** Department of Energy and Electrical Engineering, Suresh Gyan Vihar University, Jaipur-302017 India

*** Department of Mechanical Engineering, Suresh Gyan Vihar University, Jaipur-302017, India

****Department of Research and Development, Suresh Gyan Vihar University, Jaipur-302017, India

(mkgupta72@gmail.com, kks.ramky@gmail.com, rahul.aero001@gmail.com, mkbanerjee@hotmail.com)

‡ Corresponding Author; Third Author, Department of Mechanical Engineering, Suresh Gyan Vihar University Jaipur-302017 (Raj.) India, Tel: +91 9680541033, rahul.aero001@gmail.com

Abstract- The present paper deals with the assessment of water treatment capacity of solar system designed with special features. Taking stock of the situation regarding portability of water in a sample water distressed state of India, it is noticed that the TDS in available water is mostly above the limit of tolerance for drinking purpose. Thus, the capability of the designed solar system in reducing TDS content and managing the other water contaminants in the region under study has been investigated. The paper studies the energy and exergy efficiencies of the solar collector and those of the solar stills. Moreover, study is conducted in cases of coupled flat plate- solar still system and standalone solar still designed for the present experimentation to qualitatively assess the efficacy of the solar water treatment system in addressing the concern for deterioration of water in respect of increase in TDS due to unwarranted mixing of RO rejects with major water resources. A critical study on the adoptability of newly designed evaporation technique is reported in the present paper. It is observed that the presently designed solar water treatment can efficiently purify the contaminated water. The results have shown the coupled system bears a slight edge in treating the polluted water over the stand-alone system.

Keywords TDS, CETP, Solar Collector, Solar Still, Solar Water treatment

1. Introduction

Water, a basic necessity for the sustenance of life, needs to be made available to every individual. To provide drinking water to each and every household, a number of schemes have been initiated by different Governments. The performance of schemes depends upon many factors such as groundwater availability, levels of coverage and consumption, water quality and institutional arrangements for operation & maintenance [1,2]. There are examples of formulation of relevant policy and launching of various programs to meet the challenge of providing drinking water to every household in the rural and urban areas [3,4]. In a water stressed region the adequacy in supply of safe drinking water is quite often confronted with the unfavorable geographic nature and climatic conditions and hence becomes an uphill task.

Water is considered fit for drinking if it satisfies various stipulated water quality parameters. Out of those parameters, TDS is a crucial determinant of water quality in Rajasthan, India's experimental state. Total Dissolved Solids (Salts) is a concentration of positively charged and negatively charged ions in water. It originates from natural sources, sewage, urban run-off, industrial wastewater and chemicals used in the water treatment process. Referring to IS: 10500standard[6] of drinking water quality, the Total Dissolved Solid (TDS) in water should not be more than 500 mg/l. Water is unfit for human consumption, if it contains a TDS level of more than 1000 mg/l. If the drinking water contains very high TDS, several life-threatening diseases can occur. Consumption of TDS water for longer period, leads to chronic health problems viz. cancer, kidney failures, nervous system disorders, liver problems, immunity loss [5].

Even for plantation and agriculture purposes, its value should not exceed 2100 mg/l. However, due to natural and man-made reasons, the TDS may remain far above the permissible values. Apart from adversity in human health, the yield of agriculture crops has suffered a drastic decline. Moreover, the crop pattern has also changed in the last three to four decades. Several studies have suggested there should be national level initiative for supply of drinking water of acceptable quality to all the inhabitants of any water stressed

states [6-8]. Many where, the efforts are made to treat the water at the centralized and decentralized level for the supply of safe water. In spite of efforts from various authorities, it is yet to be made possible to overcome the crisis of safe drinking water for all. Therefore, adequate technological intervention cannot be postponed to any later date. [9,10].

With the evolution of advanced water treatment technology, bringing down the high TDS water to the potable level is possible. The widely used membrane technology take recourse to reverse osmosis (RO) and can bring down the TDS level from as high20,000 mg/l to the level of permissible limit, 500 mg/l. In general, the RO processes reject 20-50% of input water as waste and quite obviously the RO rejects contain a very high TDS composed of various salts. The TDS of RO reject can be as high as 20,000mg/l. This high TDS water from RO-Reject is highly detrimental to the soil and ground water, unless it is discharged scientifically after proper treatment [11]. It appears worth to evaporate the RO-Reject water or similar water of high TDS content to get pure water; on the other hand, the residue solids, depending upon its nature, need to be handled under suitable solid waste management protocol. The use solar radiation can gainfully accomplish the evaporation of high TDS water. It is anticipated that the high TDS water can be converted into potable drinking water at decentralized and centralized levels.

However, the availability of solar radiation is an important consideration for the design of solar thermal system. To alleviate this consideration, the authors have selected regions where the direct normal incidence is quite high in the present study on waste water treatment by solar radiation. As stated, the study is conducted at Jodhpur district where solar radiation is abundant; the direct normal irradiance at the experimental location is 5~7 kWhm^2, and hence is quite suitable for the installation of high efficiency Solar water treatment system may consist of a solar collector and solar still. Many types of solar technology for treatment of high TDS water are documented in literature [12-14]. While there are a number of design features being under continual change, limited effort is made on the use of parallel piping system in a Flat Plate Solar Collector (FPSC). Again, there are other scopes of alteration of design features. One such important area that warrants scientific attention is the inter-pipe spatial distance which when properly fixed in a design, can make the solar system more efficient Thus, the present study aims to design a new solar water treatment system and to examine the efficacy of using the designed solar system in treating high TDS water irrespective of its source. A solar collector of such type was designed for the present study that can exhibit high energy efficiency. Since the output of the collector determines its capacity to perform in respect of high TDS water treatment, the efficiency of a solar collector to be used for solar evaporation technology appears to be the major determinant of the suitability of the technology for waste water treatment. Thus, augmentation of efficiency of the collector is attempted for effective waste water treatment. Therefore, it appears prudent to conduct elaborate study on the effect of various factors on the efficiency of the presently designed flat plate solar collector

and that of the newly designed solar still under the available condition of solar radiance and TDS content water to treat [15].

Simple design, minimal installation costs, and autonomous water production are just some of the advantages of solar distillers like this one, which are also very easy to maintain[16-18]. However, they also have a number of disadvantages, including low efficiency, salt, scale, and rust buildup. The water should not be heated in a well built system. In order to avoid low heating the heat losses from the panels and tank should be minimised. However, at the low intensity of the sun it gives the low result of the system[19-20].

2. Experimental methods

The effectiveness of using solar energy as a means for high TDS water treatment was examined by using a flat plate solar collector preceding a solar still. The experimental arrangements are shown in Figure 1. The solar collector and solar still used in the present study are newly designed. A flat plate solar collector with modified piping is used. The design features of solar still also follow from the theory of heat transfer. The design parameters are provided in Table2 and Table 3. Salty water was used for the evaporation study by the designed solar water treatment system and final yield of distillate as well as its quality of water was assessed. The inlet temperature, intensity of available solar radiation, that is the time in a day and the mass flow rate were varied within predetermined range to find out the system capability. A Rotameter was used for mass flow rate measurement which was calibrated by volumetric method. In this method, time to fill a container of known volume was measured.

Moreover, to measure the temperatures K-type thermocouples were used. Mass of water to be treated in solar still was also varied to gather information about the capacity of the system under varying conditions. The effect of mass flow rate on the collector efficiency and pressure drop were studied by following the technique described in subsequent sections. The efficiencies of the solar collector and that of the solar still were calculated under different experimental conditions. After calculating the entropy growth and exergy efficiency as function of mass flow rate, the final performance analyses of Solar Still was carried with or without the use of Flat Plate Solar Collector designed for the present study. A finite measurement error ought to occur in real time experimentation and this was estimated by using the method due to Moffat [21]. In general, the reportable value of an experimental parameter is based on a number of measurements. In consideration of inevitable error creeping in an individual measurement the overall uncertainties in the derived values of an experimental parameter is obtained by the root of the sum of squares of error in individual measurement that is,

$$W = \left[(x_1)^2 + (x_2)^2 + \ldots\ldots\ldots\ldots\ldots\ldots + (x_n)^2 \right]^{1/2}$$

Where, x_1, $x2$… x_n are errors in individual measurements; the uncertainties in measurement are considered for all the experimentally determined parameters and are furnished in Table.1.

Table 1. The uncertainties during the measurements of the experimental parameters

Variable	Uncertainty value (%)
water inlet temperature	±0.20
water outlet temperature	±0.20
Hot inlet temperature	±0.20
Hot outlet temperature	±0.20
Mass flow rate	±2.8
Hot side mass flow rate	±2.8
Inlet side differential pressure	±2.5
outlet side differential pressure	±2.5
Friction factor measurements	±2.0
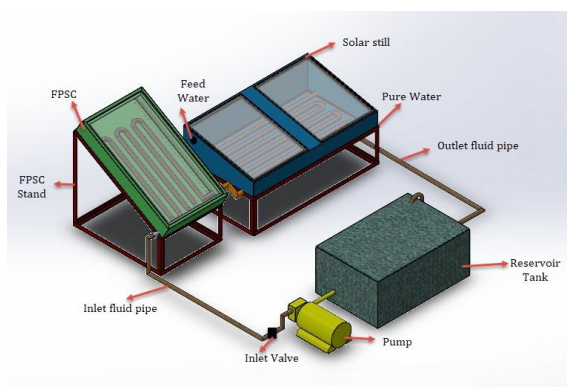
Fig. 1: Experimental set-up of FPSC and solar still

3. Results and Discussions
a. Performance of Flat Plate Solar Collector Design Features:

The solar collector is designed and fabricated by us; similarly, the solar still used in this investigation is also designed in-house by the authors. The design parameters of solar collector are furnished in Table2, whereas those of the solar still are reported in Table3. We also coupled the designed solar collector with the solar still to see if extra advantage in terms of energy efficiency is realizable or not (Fig.1). The parallel piping is employed so that higher pressure drop can be created at a higher mass flow rate. This is expected to improve the system's efficiency in respect of the system's final yield. The solar still is designed to enable getting a higher yield of treated water. The inter-pipe spatial distance is altered to maximize the system's thermal efficiency. The results are obtained from the designed system are discussed in the following sections; the process parameters are altered and the response variables are measured to find the energy and exergy efficiency of the system.

Table 2: Specification of FPSC and its component

Specification	Dimension	Units
Collector occupied volume	60×45×10	cm3
Absorption area	0.27	m2
Number of glazing plate	1	
Gap between tube	5	cm
Glazing Thickness	2.5	mm
Collector tube outer diameter	10.5	mm
Collector tube inner diameter	8	mm
Back insulation thickness	3.5	cm
Conductivity of back insulation	0.047	W/mK
Length of the pipe	4.22	m
Angle of inclination of FPSC	28	degree

The effect of mass flow rate of the fluid on the temperature of water is expected to be appreciable. Fig. 2 shows the variation of the temperatures of the tank, inlet temperature and the outlet temperature. It is observed that the increasing mass flow rate in the present case of parallel piping with changed diameter has increased the friction, for which the fluid temperature rises adiabatically. Higher mass flow rate leaves less scope for heat loss through convection and radiation. Therefore, increasing flow rate tends to increase the outlet temperature; increased outlet temperature of fluid passing via solar still is apt to raise the fluid temperature in the reservoir tank. Thus, the increased temperature at tank increases the inlet temperature by default. This effect is reflected in Fig.2. The heat content of the flowing fluid is higher at a specific temperature and therefore the loss in thermal energy becomes less while passing through the bends of parallel pipes at a higher flow rate. So, the decrease in fluid temperature is rather less and a greater extent enhances outlet temperature than the rate of rise in inlet temperature. Since the fluid is recirculated, the temperature of the tank gradually builds up which tantamount to rise in inlet temperature.
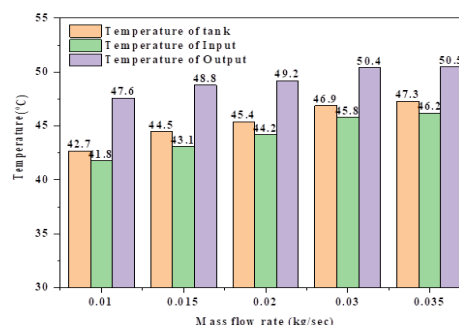
Fig. 2: Variation of mass flow rate and various Temperature

Collector efficiency can be defined as the ratio of useful energy to the incident total energy on the collector plate. The efficiency is influenced by various parameters viz. product of glazing's transmittance, absorptance of absorbing plate, intensity of solar insolation.

For a case of direct normal incidence, the efficiency of a flat plate collector is given by

$$\eta = F_R\left[\tau_0.\alpha_o - \frac{U_L\left(T_i - T_a\right)}{I_t}\right]$$

Where, F_R, τ_0, and α_0 are constants; however, changing mass flow rate the value of F_R can be changed in accordance with the following equation for F_R, which is seen to depend also on U_L, the total heat loss coefficient,

$$F_R = \frac{\dot{m}C_P}{A_C U_L}\left[1 - \exp\left(-\frac{U_L F' A_C}{\dot{m}C_P}\right)\right]$$ [22]

where F' is the collector efficiency factor and measured by the ratio of actual useful heat collected and the useful heat collected when the collector is at the local fluid temperature, T_i and T_o are the initial and final temperature. It is to be noted that change in mass flow rate leads to a decrease in initial temperature thereby enhancing the magnitude of T_i-T_o and hence there is an overall decrease in energy efficiency [Fig.3]. UL stands for the total heat loss coefficient and is given by

$$U_L = U_t + U_b + U_e$$ [17]

The top loss coefficient, U_t can be calculated by using the following formula, the Klein correlation [23],

$$U_t = \left\{\frac{\frac{1}{N}}{\frac{C}{T_P}\left[\frac{T_P - T_a}{N+f}\right]^{0.33} + \frac{1}{ha}}\right\} + \left\{\frac{\sigma(T_P + T_a)(T_P{}^2 + T_a{}^2)}{\varepsilon_P + 0.5N(1-\varepsilon_P) + \frac{2N+f-1}{\varepsilon_g} - N}\right\}$$

Where,

$$C = 365.9 \times (1 - 0.00883\beta + 0.0001298 \times \beta^2)$$

$$f = (1 + 0.04h_a - 0.0005h_a{}^2) \times (1 + 0.091N)$$

N is the number of glazing plates which is 1 in the present case; β is the azimuthal angle and is fixed for India as57⁰. $h_a = 5.7 + 3.8 V$ (V is a wind velocity derived from instantaneously, available meteorological data). Loss of heat from the back of the plate hardly exceeds 10% of the front surface loss. To find the bottom loss coefficient we use the following relation:

$$U_b = \frac{k_b}{x_b}$$

Typical values of the heat loss coefficient ranges from 0.3 to 0.6W/m²k.s [24]; similarly, the heat loss coefficient from the collector edges can be determined from relation:

$$U_e = U_b\left(\frac{A_e}{A_c}\right),$$

A_e is the area of edge area of collector and A_c is the collector area.

In a general case, when the angle of incidence is not 90°, the thermal efficiency of the collector is given by [25],

$$\eta_\theta = K_\theta F_R\left[(\tau_0.\alpha_0) - \frac{U_L\left(T_i - T_a\right)}{I_t}\right]$$

Where, K_θ is known as incident angle modifier and is given by [26],

$$K_\theta = 1 - b_0\left(\frac{1}{\cos\theta} - 1\right) - b_1\left(\frac{1}{\cos\theta} - 1\right)^2$$

For a single glaze collector, we can neglect higher order term and may use a single order equation with b0=0.1

$$K_\theta = 1 - b_0\left(\frac{1}{\cos\theta} - 1\right),$$

The θ is the flat plate collector's angle with respect to horizontal plan and is 28⁰. Experimental observations were performed both in outdoor (natural) and indoor (solar simulator mode). In order to establish comparative advantage of modified collector, indoor testing is more reliable to minimize effect of fluctuating environmental conditions Instantaneous efficiency is proportional to increase in intensity of solar radiation and also on its inclination with collector's absorbing surface. Between 12 AM to 1PM dynamic efficiency of the collector is steady and is highly efficient working time zone in month of October in India. The present experiment is conducted within 11 am to 2.30 pm. So, calculation of collector efficiency is accomplished by measurement of T_i, T_o and U_L at different mass flow rate and under the assumption of near normal incidence of solar radiation. The results are shown in Fig.3. It is observed from Fig. 3 that with increasing mass flow rate the efficiency of the collector decreases. This is because the increasing mass flow rate causes a decline in the magnitude of initial temperature and therefore, there will be net decrease in efficiency as is evident from the equation governing the efficiency of a flat plate solar collector. The observation in Fig.3 follows from the Newton's law of cooling, according to which, the rate of cooling is proportional to the temperature difference between the plate and the working fluid in the tube. As temperature difference decreases heat transfer from absorbing plate to the working fluid decreases and hence thermal efficiency of collector diminishes.

Again, the pressure drop can be written as

$$\Delta p = f\frac{\rho V^2}{2}\frac{\Delta l}{d} + k\frac{\rho V^2}{2},$$

k is the flow velocity constant, f= Friction factor, for laminar flow .

$$f = \frac{64}{Re}$$
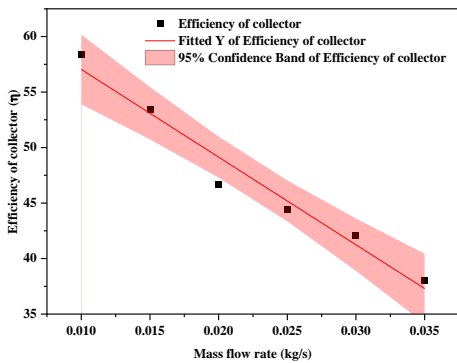
Fig. 3: Variation of mass flow rate and efficiency of collector

The variation of instantaneous efficiency of collector with the time in a day between 11 am to 2.30 pm is shown in Fig. 4. Instantaneous efficiency is measured as a function of hour in a day by keeping all other factors constants. As the time passes from 11 am it is expected that insolence will gradually increase till 12.30 pm and this increases the magnitude of It value tends to lower the second term in the equation.

$$\eta_\theta = K_\theta\, F_R \left[(\tau_0 \cdot \alpha_0) - \frac{U_L\,(T_i - T_a)}{I_t} \right].$$

It is apparent that the implication of increase in It is the increase in collector efficiency. This continues till 12.30 pm whence the angle of incidence of solar radiation becomes dominant in the intensity equation. It is noticed from the expression of K_θ that, away from the angle of incidence of 900 w/m², the value of cosθ increases and hence K_θ will decrease, So the efficiency will decrease. For this reason, we can see that the collector's efficiency decreases beyond 12.30pm shown in Fig.4.
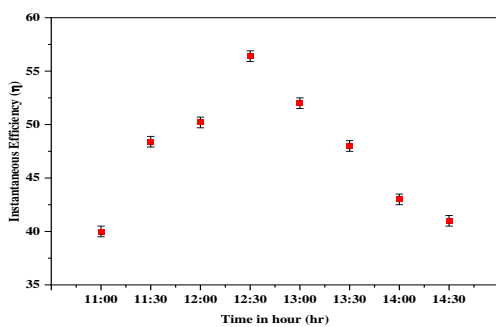

Fig 4: Variation of Time in hour and instantaneous efficiency

Fig. 5 depicts the comparative pressure drop due to flow of water through a conventional collector.Pressure drop can be calculated by using equation,

$$\Delta p = f\, \frac{\rho V^2}{2}\, \frac{\Delta l}{d} + k\, \frac{\rho V^2}{2} \; ;$$

Here V is the velocity of the fluid inside the pipe and is determined from mass flow measurement.The relation between mass flow rate and pressure drop can be calculated by the equation $\Delta p = \frac{\dot{m}^2}{2\rho A^2}\left[\frac{f\Delta l}{d} + k\right]$ The increase in flow velocity is equivalent to increase in mass flow rate.The above equation shows that increasing mass flow rate causes a higher pressure drop. On the basis of experimental results with varying mass flow rate the pressure drop was measured. The experimental results are furnished in the form of graph in Figure 5 that clearly shows the trend of increasing pressure drop with increase mass flow rate.
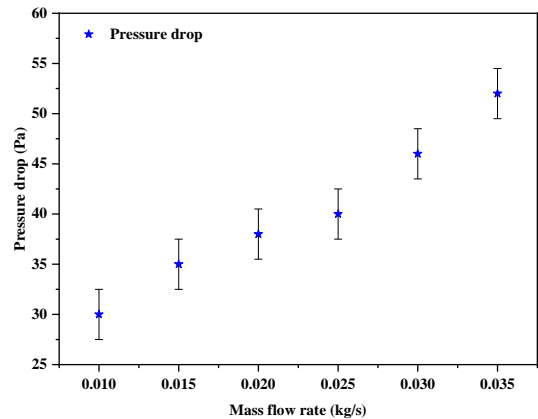

Fig. 5: Variation of pressure drop with mass flow rate

Entropy losses are of very important consideration in heat trasfer problems in the concerned systems. Entropy generation occures due to pressure losses, heat transfer from system to surroundings and irreverisble frictional heat generation.Thermodynamic treatment reveals that the entropy loss can be estimated with the help of the equation.

$$\Delta \dot{s}_{gen} = \left(R\ln\frac{p_{out}}{p_{in}} + c_p\ln\frac{T_{in}}{T_{out}} + c_p\,\frac{T_{out} + T_{in}}{T_a} \right)\Delta\dot{m} + G_c\,A_c\,(\tau\alpha)\frac{\Delta T}{T_a^2} +$$
$$\dot{m}c_p\left(\frac{1}{T_{out}} + \frac{1}{T_{in}} + \frac{2}{T_a} + \frac{(T_{out} + T_{in})}{T_a^2}\right)\Delta T + \dot{m}R\left(\frac{1}{p_{out}} + \frac{1}{p_{in}}\right)\Delta p$$
$$+ A_c\,(\tau\alpha)\left(\frac{1}{T_s} + \frac{1}{T_a}\right)\Delta G_C$$

It is observd from the above equation that the entropy loss is a function of mass flow rate. In the present experiments the mass flow rate has been varied within 0.01 kg/sec to 0.035 kg/s . The temperature and pressure parameters parameters governing the said equation are measured. R is gas constant Cp is specific heat at constant pressure, Ac is collector area and ΔGc is the global radiation.

Fig. 6 demonstrates that entropy growth increases with mass flow rate . The increase in entropy growth follows from the fact the increasing mass flow rate leads to higher pressure drop which in turn faces higher frictional resistance and adiabatic heating. This leads to entropy growth in positive direction. It is observed from Figure 6 that with increase in mass flow rate, the entropy grwth rate increases. This follows from the expression for entropy generation which reveals the the positive effect of mass flow rate in increasing the

quantum of entropy generation. The entropy growth analysis is a strategy to maximize the performance of diverse thermal systems by studying the relevant irreversibilities of the system. This study gives a short assessment of the entropy production analysis done for diverse solar thermal energy systems including solar collectors, solar heaters, solar heat exchangers, and solar stills. The mathematical concept and the formulae for calculating the entropy growth are briefly provided. Moreover, important passive approaches like the employment of nanofluids, porous materials, and inserts which are utilized to increase the efficiency of different solar systems are described. It is proven that employing entropy growth minimization approach is an efficient tool to identify the best design of solar systems.
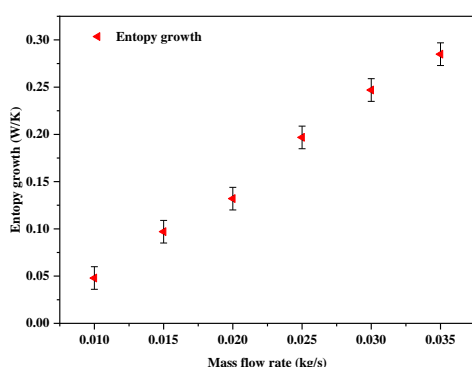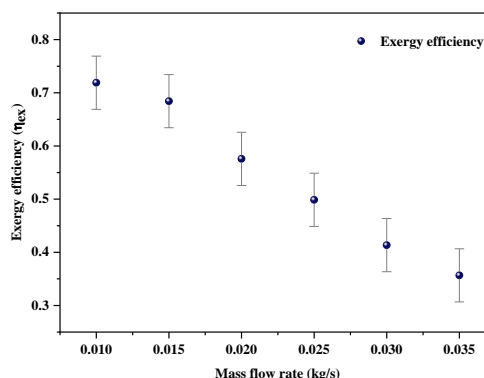

Fig 6: Variation of mass flow rate and entropy growth

In contrast, the exergy efficiency explains how a system is capable to convert available energy into useful work. For collector, the useful work is equivalent to the energy carried away by working fluid and stored in hot tank. Exergy efficiency is reciprocal to growth in entropy. Exergetic performance of the system is an indicator of system's response in terms of its ability to convert the available energy into useful work. It follows from the thermodynamics that the exergy efficiency can be given by the expression.

$$\eta_{ex} = 1 - \frac{T_a S_{gen}}{\left[1 - \frac{T_a}{T_s}\right] Q_s}$$

where, T_a, T_s are the temperatures of ambiance and sun which is 5700 K, S_{gen} is the entropy generated and Qs is the total rate of exergy received by the collector from the solar radiation. It is given by the equation $Q_s = I_t(\tau\alpha)$ where, it is the insolation on the inclined glazing surface and A_c is the collector area. The equaion for efficiencty of exergy shows a decline in the value of its efficiency with increasing entropy generation. In view of the fact enropy growth occurs with increased mass flow rate, the same tends to lower the exergy efficiency as evident in Fig. 7.

Fig 7: Variation of mass flow rate and exergy efficiency

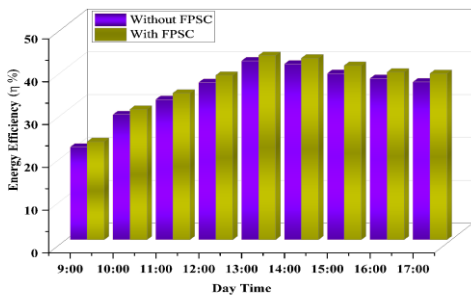**b. Performance Analysis of Solar Still**

The dimensional details of the solar still used for the present study is given in Table 3. The current study is based on the use of the above designed solar still with or without a flat plate solar collector attached to it. In both the cases, the solar radiation and the temperature are seen to change as usual as the time passes through the day. The temperature rises initially as the day progresses toward noon and falls beyond that towards sunset time. The temperature of the advanced solar still (ASS) that is the one with FPSC is found to be higher than that without FPSC. The ASS has a higher absorption capacity for solar radiation. In this case, the evaporation rate of water is higher; it also exhibits better condensation. ASS was found to perform better than conventional ones because of such increased evaporation rate with enhanced condensation

Table 3: Specification of Solar still and its component

Specification	Dimension	Units
Length of the solar still	120	cm
Width of solar still	65	cm
Absorption area of solar still	0.78	m^2
Inclination of glazing plate	15	degree
Glazing Thickness	2.5	mm
Collector tube outer diameter	10.5	mm
Collector tube inner diameter	8	mm
Back insulation	3.5	cm

thickness		

The efficiency of solar still is obtained from $\eta = \frac{\sum m_{cf} \times h_{fg}}{\sum I_t \times A_s \times 3600}$ where, I_t is insolence and A_s is the area of solar still; m_{cf} is the collected mass of fluid and h_{fg} represents the total enthalpy of the fluid-gas system. In most solar stills, paint is used to absorb sunlight and raise the temperature of the water. The black chrome paint mixed with nanomaterial has been used in our experiments for a better absorption of solar radiation by the solar still. The presently used ASS is found to have 13.4 percent more evaporation and condensation rate than the other experimental solar still. The energy efficiency of the presently used solar still is shown in Figure 8. It is observed from the figure that attaching a flat plat collector to the solar still has increased the energy efficiency of solar still; however, the improvement is rather marginal. As is expected the efficiency increases continuously till 13.30, beyond which, it gradually declines to a lower value. It may be noted that in the case of experimental location (Jodhpur, India known as Sun city), the abundance of solar radiation till 17pm enables to record a reasonably good energy efficiency of solar still. The maximum efficiency of ~45% at 13.30 pm decreases to a value of 40% at 17.00 pm to mean that the solar evaporation technology acts quite efficiently with satisfactory energy efficiency over a good length of time shown in Fig. 8.

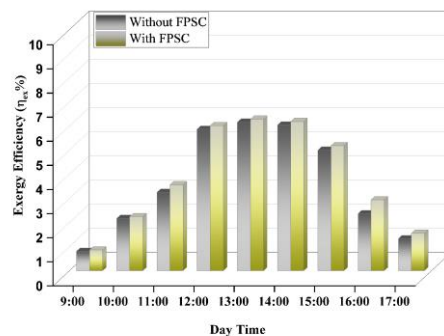**Fig 8:** Variation of energy efficiency with progressing time in a day

c. **Exergy Analysis of Solar Still**

The work, a system needs to perform, before being brought to thermodynamic equilibrium is known as the exergy of the system. The exergy analysis is treated as complimentary to energy analysis as the sustainability of a system is greatly determined by exergy analysis. Exergy analysis has been carried out in the present study for identification of the causes of process inefficiencies; moreover, it aids in understanding the magnitude of the inefficiency of a process so that the corrective actions can be taken at the right locations. An insolation formula, as given below, has been used to express the exergy input to a solar still [26,27].

$$Ex_{input} = I_t \times A_s \left[1 - \frac{4}{3} \times \left(\frac{T_a}{T_s} \right) + \frac{1}{3} \times \left(\frac{T_a}{T_s} \right)^4 \right];$$

T_s is the temperature of solar still, a measured quantity. However, the hourly exergy output is measured by the equation, $Ex_{output} = \frac{m_{cw} \times h_{fg}}{(3600s.h^{-1})} \times \left(1 - \frac{T_a}{T_w} \right)$. T_a and T_w denote the ambient temperature and the temperature of water respectively. By, definition, the ratio of exergy output and exergy input gives the efficiency, viz. $\frac{Ex\ output}{Ex\ input}$. The temperature parameters in the above two equations are measured at different time interval within a day and making use of the data, the exergy efficiency of solar still designed for the present investigation is calculated at one hourly interval between 9.30 am and 5.30 pm. The results are furnished in Figure9, which shows the change in exergy efficiency for both cases of (i) solar still with FPSC and (ii) that without the flat plate sola collector. It is observed that as the time progresses towards noon, the exergy efficiency increases for the both the types of set up, reaches a maximum at 13.30pm and beyond this, the exergy value decreases due to reducing insolence. So far as exergy efficiency is concerned, the benefit of coupling solar still with FPSC is very marginal.

Fig 9: Variation of exergy efficiency with time advancement in a day.

It is apparent from the foregoing discussion that the design efficiency of the flat plate collector and that of solar still have been assessed by monitoring the energy as well as exergy efficiencies of the solar collector and solar still. While determining the efficacy of the presently designed solar still, both the cases of solar still coupled with FPSC and that without FPSC have been considered.

The study is further extended to examine the real-life performance in respect water purification. Experiments are conducted by the evaporation technology setup designed in the present investigation (Fig. 1) to probe into the capability of the designed system in treating the polluted water. For the purpose of the study water from three different sources were taken. The physico-chemical characteristics of water used for the present experimentation are furnished in Table 4. The same table shows the final outcome of solar distillation by

the designed setup. It is evident that after solar distillation, all the harmful minerals are completely removed and their individual value has become zero. Moreover, the process has ably adjusted the pH value of the treated water. Both acidity and alkalinity are removed from the water which shows a pH value of 6.8-7.2. This is indicative of the occurrence of effective treatment of heavily contaminated water.

Table 4: Test Report of different water distillation

Physio-chemical characteristic	Feed Water (Before Distillation)			Solar Distillation (after solar distillation)
	Basin Water	Kitchen Water	Muddy Water	
PH	8.2	8.8	5.2	6.8 – 7.2
Total Solid(mg/l)	923	1332	1421	00
TDS	700	880	316	00
TS	210	452	617	00
Sulphate	168	254	216	00
Phosphates	151	176	162	00
Chloride	194	233	212	00

4. Conclusion:

The authors wish to conclude that the designed flat plate collector yields maximum instantaneous energy efficiency at 12.30 pm reaching a value, as high as 57% or more. The retaintivity of energy efficiency is also high as the efficiency is above 40% till 2.30pm. The energy efficiency of the collector decreases with increasing mass flow rate. Increasing mass flow rate leads to an increase in pressure drop, and as a result of this the entropy generation is enhanced with concurrent decrease in exergy efficiency. These observations are in agreement with laws of classical thermodynamics. It is further concluded that the energy efficiency of the designed solar still is as high as 45% or more at around 13.30 pm beyond which it gets slightly reduced retaining an efficiency of 40% till 17.00 pm. It is also concluded that the exergy efficiency of solar still is maximized at 13.30 pm. Moreover, the authors infer that the gain of coupling FPSC with solar still in respect of energy efficiency is rather marginal when compared with the performance of standalone solar still, designed in the present investigation. The authors also conclude that the designed setup is extremely efficient in solar distillation of contaminated water with the final yield of neutral water without any contamination. This entices the authors to advance the inferring statement by saying that the presently designed advanced solar still (FPSC coupled) is effective in waste water treatment irrespective of its origin, industry or community.

References

1. S. K. Verma, A. K. Tiwari, and D. S. Chauhan, 'Performance augmentation in flat plate solar collector using MgO/water nanofluid', Energy Conversion and Management, vol. 124, pp. 607–617, 2016, doi: 10.1016/j.enconman.2016.07.007.

2. M. Hatami and D. Jing, 'Optimization of wavy direct absorber solar collector (WDASC) using Al2O3-water nanofluid and RSM analysis', Applied Thermal Engineering, vol. 121, pp. 1040–1050, Jul. 2017, doi: 10.1016/j.applthermaleng.2017.04.137.

3. W. Kang, Y. Shin, and H. Cho, 'Economic Analysis of Flat-Plate and U-Tube Solar Collectors Using an Al2O3 Nanofluid', Energies, vol. 10, no. 11, Art. no. 11, Nov. 2017, doi: 10.3390/en10111911.

4. N. K. C. Sint, I. A. Choudhury, H. H. Masjuki, and H. Aoyama, 'Theoretical analysis to determine the efficiency of a CuO-water nanofluid based-flat plate solar collector for domestic solar water heating system in Myanmar', Solar Energy, vol. 155, pp. 608–619, Oct. 2017, doi: 10.1016/j.solener.2017.06.055.

5. J. Liu, Z. Ye, L. Zhang, X. Fang, and Z. Zhang, 'A combined numerical and experimental study on graphene/ionic liquid nanofluid based direct absorption solar collector', Solar Energy Materials and Solar Cells, vol. 136, pp. 177–186, May 2015, doi: 10.1016/j.solmat.2015.01.013.

6. T. Yousefi, F. Veysi, E. Shojaeizadeh, and S. Zinadini, 'An experimental investigation on the effect of Al2O3–H2O nanofluid on the efficiency of flat-plate solar collectors', Renewable Energy, vol. 39, no. 1, pp. 293–298, Mar. 2012, doi: 10.1016/j.renene.2011.08.056.

7. M. Faizal, R. Saidur, S. Mekhilef, and M. A. Alim, 'Energy, economic and environmental analysis of metal oxides nanofluid for flat-plate solar collector', Energy Conversion and Management, vol. 76, pp. 162–168, Dec. 2013, doi: 10.1016/j.enconman.2013.07.038.

8. A.E.Kabeel, Mohamed A.Teamah and Gmal B.Abdel Aziz, 'Modified pyramid solar stillwith v-corrugated absorber plate and PCM as a thermal storage medium', Journal of Cleaner Production, vol. 161, pp. 881-887, Sept. 2017, https://doi.org/10.1016/j.jclepro.2017.05.195.

9. B. Madhu, E. Balasubramanian, P.K. Nagarajan, Ravishankar Sathyamurthy, A.E. Kabeel, T. Arunkumar,D.Mageshbabu 'Improving the yield of fresh water from conventional and stepped solar still with different nanofluids',Desalination and Water Treatment, vol. 100, pp. 243–249, Dec. 2017, doi:10.5004/dwt.2017.21279.

10. A. E. Kabeel, Z. M. Omara, F. A. Essa, A. S. Abdullah, T. Arunkumar, and R. Sathyamurthy, 'Augmentation

of a solar still distillate yield via absorber plate coated with black nanoparticles', Alexandria Engineering Journal, vol. 56, no. 4, pp. 433–438, Dec. 2017, doi: 10.1016/j.aej.2017.08.014.

11. P. N. Kumar, D. G. H. Samuel, P. K. Nagarajan, and R. Sathyamurthy, 'Theoretical analysis of a triangular pyramid solar still integrated to an inclined solar still with baffles', International Journal of Ambient Energy, vol. 38, no. 7, pp. 694–700, 2017, doi: 10.1080/01430750.2016.1181569.

12. H. Panchal, N. Patel, and H. Thakkar, 'Various techniques for improvement in distillate output from active solar still: a review', International Journal of Ambient Energy, vol. 38, no. 2, pp. 209–222, 2017, doi: 10.1080/01430750.2015.1076518.

13. K. Karthik, A. Manimaran, R. R. Kumar, and J. U. Prakash, 'Solar energy performance analysis of basin-type solar still under the effect of vacuum pressure', International Journal of Ambient Energy, vol. 41, no. 8, pp. 922–926, 2020, doi: 10.1080/01430750.2018.1501734.

14. H. Panchal and K. K. Sadasivuni, 'Enhancement of the distillate yield of solar still by separate and inbuilt condensers: A mini-Review', International Journal of Ambient Energy, vol. 0, no. 0, pp. 1–5, 2020, doi: 10.1080/01430750.2020.1831595.

15. P. Dumka and D. R. Mishra, 'Influence of salt concentration on the performance characteristics of passive solar still', International Journal of Ambient Energy, vol. 42, no. 13, pp. 1463–1473, 2021, doi: 10.1080/01430750.2019.1611638.

16. P. Mazidi, G.N. Baltas, M. Eliassi, P. Rodriguez, A Model for Flexibility Analysis of RESS with Electric Energy Storage and Reserve, 7th Int. IEEE Conf. Renew. Energy Res. Appl. ICRERA 2018. (2018) 1004–1009. https://doi.org/10.1109/ICRERA.2018.8566992.

17. Farrukh javed, Impact of Temperature & Illumination for Improvement in Photovoltaic System Efficiency, Int. J. Smart Grid. (2022). https://doi.org/10.20508/IJSMARTGRID.V6I1.222.G1 85.

18. A.A.-A.W.A.K. Kenneth Okedu, Electricity Sector of Oman and Prospects of Advanced Metering Infrastructures, Int. J. Smart Grid. (2022). https://doi.org/10.20508/IJSMARTGRID.V6I1.228.G1 84.

19. D. Pagnoncelli, P. Perani and E. Ragaini, "ABB Smart Lab: Simulating future applications with present equipment," 2015 International Conference on Renewable Energy Research and Applications (ICRERA), 2015, pp. 1627-1630, doi: 10.1109/ICRERA.2015.7418681.

20. F. Solak, H. Gözde, M. Akif Şenol and M. Cengiz Taplamacioglu, "Design of power control unit for heat recovery device used in renewable energy system," 2015 International Conference on Renewable Energy Research and Applications (ICRERA), 2015, pp. 1185-1189, doi: 10.1109/ICRERA.2015.7418596.

21. Moffat RJ. Describing the Uncertainties in Experimental Results. Experimental Thermal and Fluid Science. 1988;1:3-17.

22. Duffie J.A, Beckman WA. Solar engineering of thermal processes. New York: Wiley. 2006.; 3rded.

23. Klein S.A., Calculation of flat-plate solar collector loss coefficients. Sol Energy. 1979;17(1):79–80.

24. Hottel HC, Woertz BB. Performance of flat-plate solar - heat collectors. TransASME. 1942;64(91).

25. Kalogirou SA. Solar thermal collectors and applications. Progress in energy and combustion science. 2004;30(3):231-95.

26. A. E. Kabeel et al., 'Effect of water depth on a novel absorber plate of pyramid solar still coated with TiO2 nano black paint', Journal of Cleaner Production, vol. 213, pp. 185–191, Mar. 2019, doi: 10.1016/j.jclepro.2018.12.185.

27. S. W. Sharshir, A. H. Elsheikh, G. Peng, N. Yang, M. O. A. El-Samadony, and A. E. Kabeel, 'Thermal performance and exergy analysis of solar stills – A review', Renewable and Sustainable Energy Reviews, vol. 73, pp. 521–544, Jun. 2017, doi: 10.1016/j.rser.2017.01.156.